ELSEVIER

Journal of Power Sources 89 (2000) 117–124

JOURNAL OF POWER SOURCES

www.elsevier.com/locate/jpowsour

An electrochemical investigation of mechanical alloying of MgNi-based hydrogen storage alloys

Jian-Jun Jiang [a,b], Michael Gasik [b,*]

[a] *Faculty of Traffic Science and Engineering, Huazhong University of Science and Technology, Wuhan 430074, People's Republic of China*
[b] *Department of Materials Science and Rock Engineering, Helsinki University of Technology, Espoo FIN-02015, Finland*

Received 9 November 1999; received in revised form 12 February 2000; accepted 21 February 2000

Abstract

The electrochemical properties of amorphous MgNi-based hydrogen storage alloys synthesized by mechanical alloying (MA) were evaluated. The results show that these amorphous $Mg_{50}Ni_{50}$ alloys exhibit a higher discharge capacity and relatively good rate capacity at a suitable grinding time while their cycle life is very poor. In order to improve the cycle life, the surface of the amorphous $Mg_{50}Ni_{50}$ alloy was coated with Ti, Al and Zr in Spex 8000 mill/mixer and the coating effects were further investigated. Based on experimental results, two kinds of MgNi-based amorphous alloys are designed by substituting part of Mg in MgNi-based alloys by suitable elements. These alloys are then composed of four components. Thus, the cycle life of electrodes consisting of these quaternary amorphous alloys is greatly improved.

Keywords: Mg-based alloys; Amorphous; Mechanical alloying; Metal hydride electrode; Electrochemical properties

1. Introduction

In recent years, for the development of high performance hydrogen storage alloys used as active materials for the negative electrode of Ni–MH batteries, considerable attention has been paid to the research of Mg-based alloys, particularly amorphous MgNi-type alloys prepared by mechanical alloying (MA) and mechanical grinding (MG) with different raw materials. Lei et al. [1] and Sun et al. [2] synthesized it to use mainly pure cheap magnesium, nickel metal powder and MA in a planetary ball mill. Kohno et al. [3] and Kohno and Kanda [4] studied the electrochemical properties of the composite materials obtained with Mg_2Ni and Ni by MG. Iwakura et al. [5] and Nohara et al. [6] also investigated the enhancement of electrochemical characteristics of nanocrystalline Mg_2Ni and homogeneous amorphous alloys prepared by planetary ball milling of Mg_2Ni with and without Ni. Extensive studies have been carried out on the discharge capacity and cycle life of alloy electrodes under single discharge current density, e.g., discharge capacity $C_{50\ mA/g}$ at discharge current density of 50 mA/g. However, only a few publications have been devoted to the rate capacity of amorphous MgNi alloys [1].

Although amorphous MgNi-type alloys can electrochemically absorb and desorb a large amount of hydrogen at room temperature [1–5], the electrochemical degradation rate is much faster than that of AB_5 and AB_2 type alloys. Using X-ray diffraction (XRD) and XPS, Liu et al. [7] have informed that the main reason for degradation of amorphous MgNi alloy is serious oxidation of magnesium and nickel in the electrolyte. Likewise, Liu et al. [8] have investigated more than 10 different MgNi-based amorphous alloys with partial replacement of nickel by other elements (Zn, Ti, Mn, Cu) in order to improve cycle life. In spite of this replacement, the cycle life was far below the requirement for practical usage. Some results on amorphous alloy have also shown that discharge performance is strongly dependent on the surface properties altered by various surface pre-treatments. Iwakura et al. [9] have studied the electrochemical properties of MgNi alloys surface-modified with graphite. The marked improvement of discharge capacity was achieved with surface modification of MgNi alloy, but the tendency of degradation was similar to that without modification. Therefore, selection of special modifying elements for MgNi-based amorphous alloys

* Corresponding author. Tel.: +358-9-451-2775; fax: +358-9-451-2799.
E-mail address: mgasik@pop.hut.fi (M. Gasik).

0378-7753/00/$ - see front matter
PII: S0378-7753(00)00400-6

can be the main key to improve its cycle life, especially coating of elements such as Ti, Zr and Al, change surface oxide composition, and improve cycle life herewith.

In this study, the performance of amorphous MgNi alloy electrodes prepared by attrition ball milling was evaluated and the effect of surface modification on the amorphous alloys was investigated. Based on the results of these studies, various quaternary MgNi-based amorphous alloys were designed.

2. Experimental details

2.1. Preparation of MA alloys

The alloy samples were synthesized by MA with pure elemental powders of Mg (particle size 120 μm), Ni (particle size diameter 5 μm) and other metal powders (such as Ti, Zr and Al). MA was performed with an attrition mill (Simoloyer, Model CM01, Zoz) at different ball milling times in argon atmosphere. Each single cycle comprises of two kinds of milling velocity, 200 rpm for 1 h and 500 rpm for 4 h, respectively. Stainless steel balls ($\sim$ 4.7 mm) were used in the cylindrical stainless grinding chamber (700 ml). The mass ratio of steel balls to metal powder was 50:1. After completion of grinding, the sample tube was opened in a dry nitrogen atmospheric glove box to take the sample out. All the alloy samples prepared were handled in this way without exposure to air.

The modification of MgNi material is complicated because its properties are not changed significantly by substitution of Mg by other elements, on the contrary to AB_5 compounds with transition and rare earth metals. In order to perform the surface modification on the MgNi amorphous alloys, a Spex 8000 model Mixer/Mill was used. The surface of parent alloy was then only coated by the suitable element without damage to its structure [10].

2.2. Electrochemical measurement

The alloys prepared by MA were investigated by using an electrochemical charge–discharge method. Test electrodes were fabricated by compressing 0.4 g alloy mixture, produced from alloys and electrolytic copper powder in the weight ratio of 1:3, into a pellet of 10 mm diameter under a pressure of 10 MPa. The mercury/mercury oxide (Hg/HgO) electrode was used as reference electrode and platinum wire as counter electrode in 6 M KOH solution. In the charge–discharge cycle tests at 30 ± 2°C in a water bath, charge was conducted using a charge current rate of 300 mA/g for 3 h. The rate capacity of alloys was measured simultaneously using different samples from the same alloy considering the relatively fast capacity decay of amorphous MgNi alloys. All measurements were carried out using a computer-controlled battery cycler. The cut-off discharge potential was fixed at -0.6 V with respect to Hg/HgO reference electrode.

2.3. P–C–T (pressure–composition–temperature) measurement

The *P–C–T* measurements can be a useful technique in evaluating hydrogen storage alloys as electrochemical material, although gas phase storage of hydrogen does not completely guarantee that a particular material (particularly, a Mg-based alloy) is capable of storing hydrogen in an electrochemical cell. The *P–C* isotherms were measured using a Sieverts-type apparatus. About 1 g powder sample was taken for each test. The measurement was done at a constant temperature of 413 K to investigate the desorption equilibrium pressure.

2.4. XRD, scanning electron microscopy (SEM) analysis

The structures of alloy powders were characterized by XRD analysis utilizing CuKα radiation. The inspection of surface morphology was conducted using Phillips 515 scanning electron microscope linked with electron dispersive X-ray analysis (EDX).

3. Results and discussion

3.1. Effect of grinding time on the initial discharge capacity and cycle life of $Mg_{50}Ni_{50}$ alloys

In an attrition ball mill, grinding time is related to average ball diameter and agitator speed as follows:

$$t = k\frac{d}{\sqrt{n}},$$

where t is the grinding time to obtain a certain particle size, k is a constant that varies with the processed slurry, the type of medium and used mill, d is the diameter of the balls and n is shaft movement in revolutions per minute. Selection of suitable milling parameters should be taken into account because the end products of MA depend strongly upon these parameters.

Fig. 1 shows the initial discharge capacity of $Mg_{50}Ni_{50}$ alloy as a function of grinding time in an attrition ball mill. As the grinding time increases from 40 to 60 h, initial discharge capacity increases to its maximum. However, after increasing grinding time from 60 to 100 h, the initial discharge capacity decreases again. It is obvious from this figure that an optimum grinding time exists for the maximum discharge capacity.

The change of particle morphology during grinding metal powders is initially caused by microforging, fracture

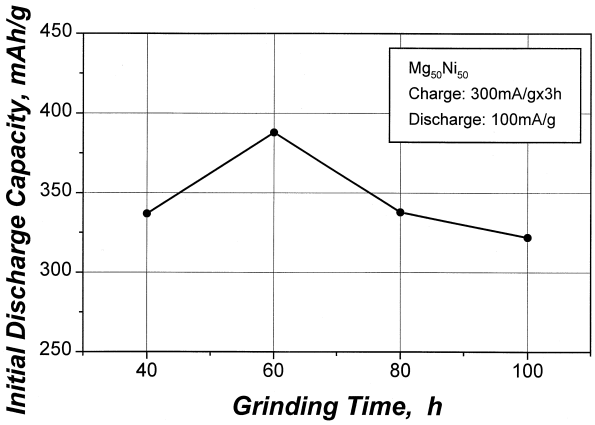

Fig. 1. Dependence of initial discharge capacity of $Mg_{50}Ni_{50}$ alloy on grinding time of attrition ball mill process.

and eventually by agglomeration. The SEM results for morphology of alloys ball-milled during 60 and 100 h are shown in Fig. 2. In Fig. 2a, it can be seen that most $Mg_{50}Ni_{50}$ alloy particles after 60 h of ball milling are smaller than 10 μm in size. Fig. 2b also clearly indicates that after 100 h grinding time, the alloy is agglomerated by welding and mechanical interlocking of spongy or rough surface. A different grinding time does not bring about a change of the amorphous microstructure as proved by the XRD, as seen in Fig. 3. In addition, elemental analysis carried out by EDX shows that the bulk of alloy is uniform and the composition of larger particles and of the others obtained after different grinding time is the same. However, the initial capacity decreases as agglomeration of large particles occurs by overtiming the optimum grinding time. Decreasing discharge capacity is caused by significantly decreasing active surface area of very large particles with a diameter over 100 μm.

Usually, the gaseous hydrogen storage capacity of an alloy is known as the indicator of the upper electrochemical energy density limit in an electrochemical cell. The *P–C* isotherms of hydrogen absorption and desorption for the $Mg_{50}Ni_{50}$ alloy ball-milled during 60 and 100 h at 140°C are shown in Fig. 4. As seen in this figure, the *P–C* isotherm of the as-ball-milled state exhibits no plateau at all because of the internal strain and chemical disorder. The gaseous hydrogen absorption capacity of the alloy ball-milled during 60 h is higher than that of the alloy ball-milled during 100 h. This result is in good agreement with the behavior of discharge capacity for electrodes (Fig. 1) fabricated with the same alloys.

The effect of grinding time on the cycle life of amorphous $Mg_{50}Ni_{50}$ alloys is shown in Fig. 5. It is clearly seen that the discharge capacity decreases rapidly with increasing cycle number. This is caused by preferential selective magnesium oxidation in the highly corrosive 6 M KOH electrolyte. Longer grinding time has only little influence on the cycle life of ball-milled amorphous alloys.

3.2. Rate capacity of amorphous $Mg_{50}Ni_{50}$ alloys

Amorphous MgNi alloy prepared by MA needs no additional activation process unlike the AB_5 and AB_2-type hydrogen storage alloys. This is advantageous in commercialization. Fig. 6 shows the rate capacity change of amorphous $Mg_{50}Ni_{50}$ alloy electrodes at a discharge current density of 20, 50, 100, 300 and 600 mA/g in the first

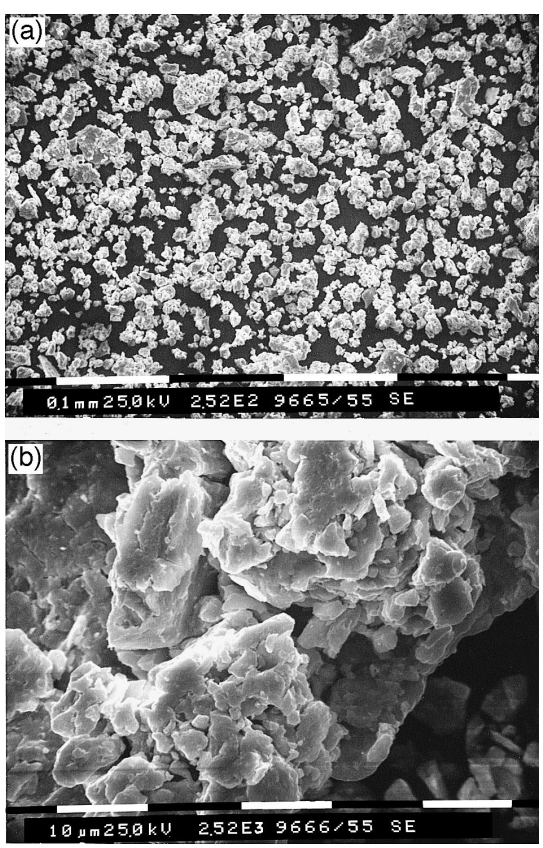

Fig. 2. The SEM morphology of $Mg_{50}Ni_{50}$ alloys with different grinding times: (a) 60 h; (b) 100 h.

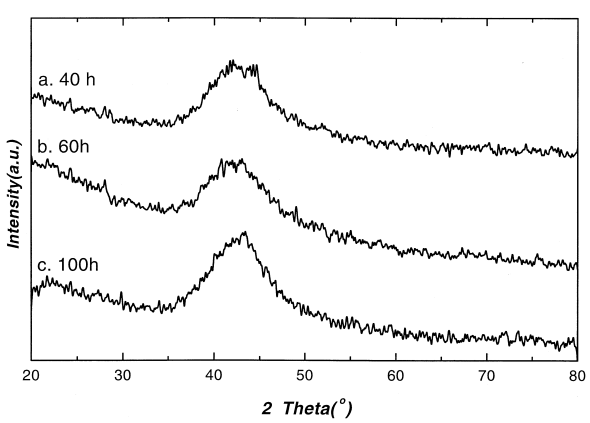

Fig. 3. The XRD patterns of $Mg_{50}Ni_{50}$ alloys with different grinding times.

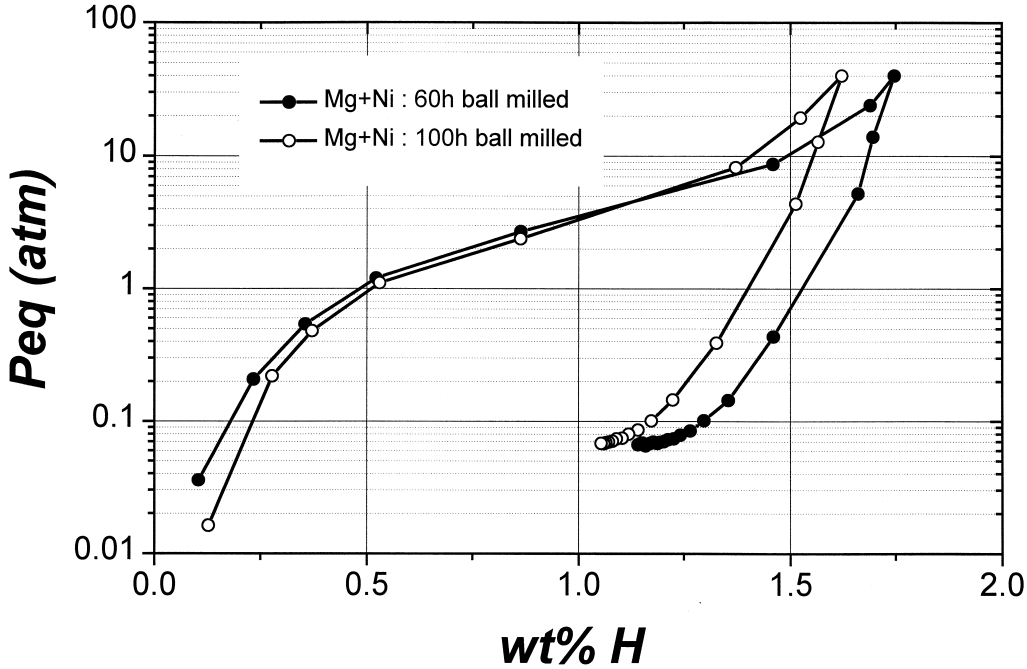

Fig. 4. The P–C–T curves of $Mg_{50}Ni_{50}$ alloys as a function of grinding time.

cycle. The discharge potentials are decreasing gradually at the end-of-discharge state for higher discharge rates (300 and 600 mA/g) and much faster for lower discharge rates (20 and 50 mA/g). This effect is generally known. By increasing the discharge rate, the rate of the charge transfer reaction increases, but there is sufficient charge (hydrogen) left in the electrode even at the end-of-discharge state because the diffusion rate of atomic hydrogen from the bulk to the surface of the MH particles is slower than the charge transfer reaction on the surface of the particle. Therefore, the potential is decreasing gradually. For the lower discharge rates, at the end-of-discharge state (cut-off voltage of -0.6 V), the hydrogen concentration within the electrode and on the electrode/electrolyte interface reaches a value close to zero because atomic hydrogen has enough time to diffuse, which causes the electrode potential to change rapidly to more positive values. However, the discharge capacity increases firstly with increasing discharge rate from 20 to 100 mA/g and then decreases with further increasing discharge rate from 100 to 600 mA/g. It indicates that a maximum capacity exists at a suitable discharge current density. This behavior, rarely found in AB_5 and AB_2-type crystalline alloy electrodes, may be explained by a fast degradation of amorphous MgNi alloys during a longer duration of the discharge process. This fast degradation of amorphous MgNi alloy can be caused by serious oxidation of magnesium. Thus, the electron transfer reaction of amorphous MgNi alloys depends strongly on oxide-covered metal hydride electrodes, not on the hydride electrode itself [11]. Reaction rates are controlled by the film thickness. In the initial charge–discharge cycling, the film is sufficiently thin so that an electron can be exchanged with the underlying alloy. During further charge–discharge cycles, the oxide film becomes thicker, acts then as barrier for electron transfer but does not provide significant corrosion protection because of its open structure [12]. For an oxide-covered alloy electrode, the exchange current density decreases strongly and even approximately exponentially with increasing oxide film thickness. As a consequence, the measured discharge capacity at low discharge current density is lower than that at high discharge current density due to long-time degradation. For an amorphous MgNi alloy, thermodynamic and kinetic degradation can be taken into consideration. The

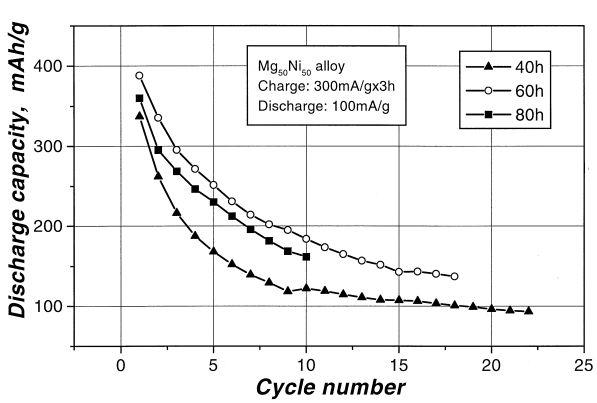

Fig. 5. Effect of grinding time on the cycle life of $Mg_{50}Ni_{50}$ alloys.

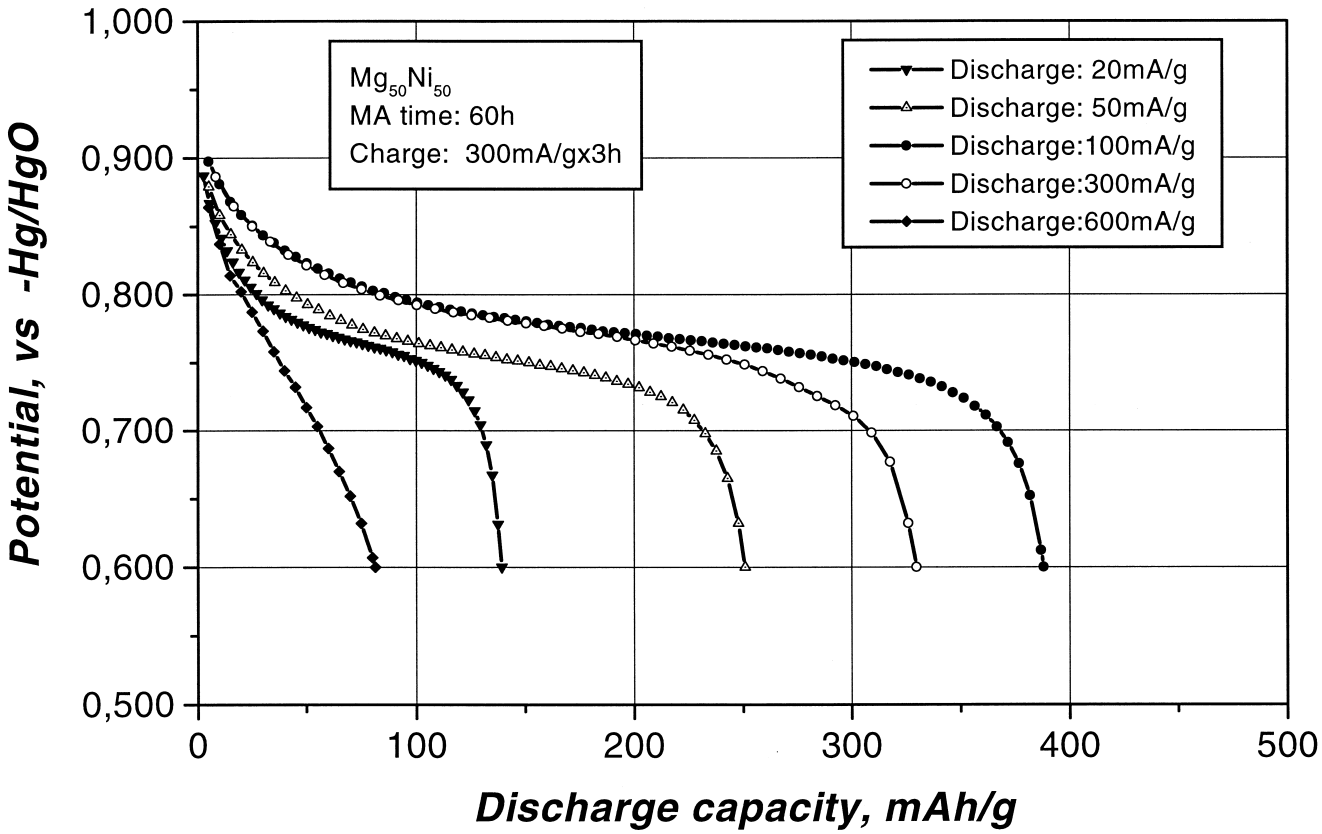

Fig. 6. Dependence of discharge potential on the rate capacity for $Mg_{50}Ni_{50}$ alloys.

behavior of thermodynamic degradation is related to decreasing the amount of the hydrogen storaging part of the alloy by oxidation of an alloying element [13]. The kinetic degradation is related to preventing fast hydrogen diffusion through an oxidized surface into or out of the bulk alloy, combined with decreasing the exchange current density of the electrochemical oxidation reaction. In general, this kinetic degradation plays a main role in amorphous alloys. A detailed analysis of degradation mechanism patterns supporting the above conclusions will be published elsewhere [14].

The rate capacity of the amorphous alloys obtained by attrition ball milling is better than that of others obtained by using a planetary-type ball mill [1]. This is due to the central rotating shaft of the attrition mill, which is equipped with several vertical arms. The motion causes a differential movement between the balls and the materials being milled. Impact and shearing force action caused by the shaft lead to more changes on the powder shape and structure. Therefore, attrition milling can provide the following good effects.

At first, the large surface-to-volume ratio in the alloy powders enhances the accessibility of the alloy for hydrogen penetration. Secondly, during the milling process, a significant amount of strain, disorder and defects is created in alloy material, which shorten hydrogen diffusion paths. Additionally, the lack of a crystallographically defined structural unit resulting from distribution of local atomic positions causes a wide distribution of available sites for hydrogen [15].

All these effects will promote the kinetics of hydrogen adsorption and desorption so that the high rate dischargeability of $Mg_{50}Ni_{50}$ alloys can be achieved.

3.3. Effect of surface modification on the cycle life of $Mg_{50}Ni_{50}$ alloys

The cycle life of the binary MgNi alloy electrode is very poor, which is a strong barrier to its practical application. It is known that magnesium hydroxide is formed easily on the alloy particles in strong alkaline solution [2] and is growing continuously because of its open structure. Thus, a surface modification must be considered, by which the thick oxide layer can be suppressed or further oxidation can be prevented and simultaneously, some catalytic surface structures can be provided.

To investigate the effect of surface modification on the cycle life, the $Mg_{50}Ni_{50}$ alloy was coated with Zr, Ti and Al by using a Spex 8000 mill/mixer. As seen in Fig. 7, Ti-, Al- and Zr coatings can improve its cycle life. Effec-

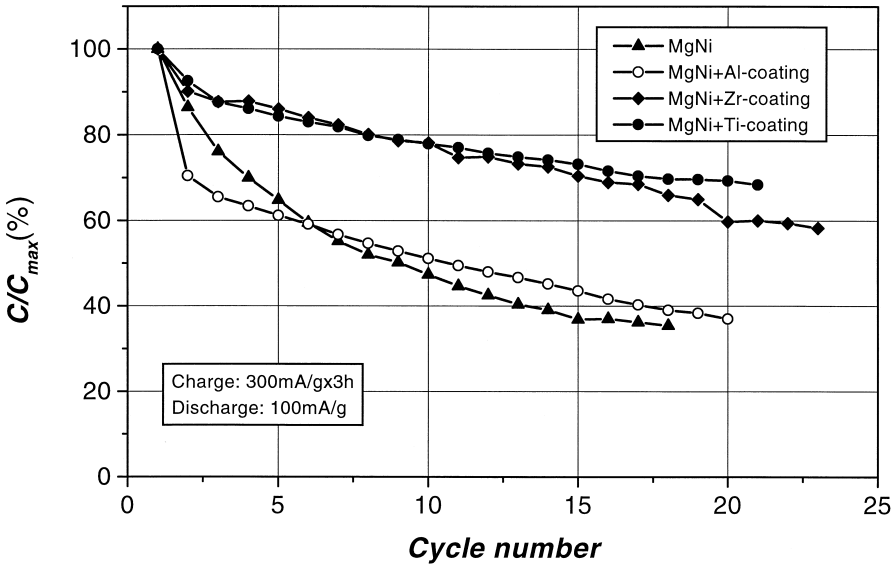

Fig. 7. Effect of Ti-, Al- and Zr coatings on the cycle life of $Mg_{50}Ni_{50}$ alloys.

tiveness in improving the cycle life of the $Mg_{50}Ni_{50}$ alloys by coating increases in the following order: Ti > Zr > Al. The improvement of cycle life is caused by selective formation and dissolution of coating element oxide on the alloy surface. Such oxide formation and dissolution decrease the corrosion rate of Mg and improve the electrochemical catalytic activity and electrochemical stability of the electrode. In the Ti-coated amorphous alloys, the improvement of the electrochemical properties will be due to selective dissolution of TiO_2 from the film on the electrode surface during charge–discharge cycles. After this selective dissolution, a porous electrocatalytically active Ni layer remains on almost the whole electrode surface. For crystalline alloys, such a selective dissolution of the oxide layer is difficult to achieve [16]. In the case of Zr coating, the zirconium oxide on the alloy surface has to be a strong barrier to hydrogen penetration [17], but it can be dissolved in strong alkaline solution [18] and then nickel in the top surface layers is enriched just as in the case of Ti coating. Therefore, Ti- and Zr coatings on alloy particles result in

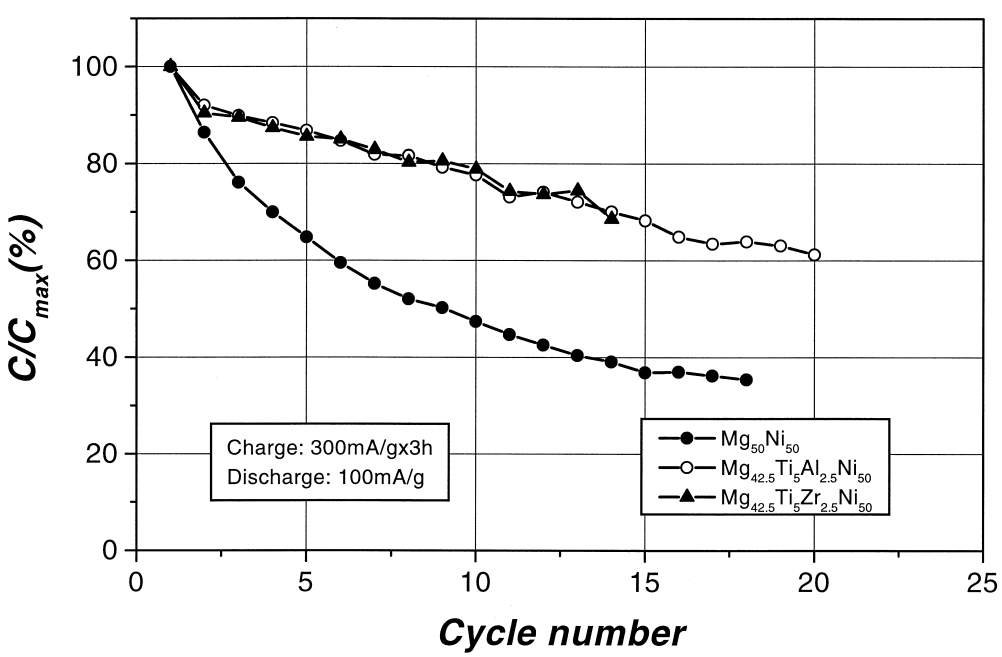

Fig. 8. Discharge capacity vs. cycle number for the $Mg_{42.5}Ti_5Al_{2.5}Ni_{50}$, $Mg_{42.5}Ti_5Zr_{2.5}Ni_{50}$ and $Mg_{50}Ni_{50}$ alloys.

an improvement of the cycle life. But oxides on the alloy surface, formed from coating elements, increase the electrochemical polarization of hydride electrodes and hence, decrease the discharge capacity of alloys. Consequently, Ti- and Zr coatings on the alloy surface result in an improvement of the cycle life, but a lower discharge capacity.

In contrast to Ti- and Zr coatings, Al coating causes a somewhat anomalous behavior of the initial discharge capacity. During early charge–discharge cycling, the strong oxidation tendency of Al will form a passive film stable against the electrolyte and therefore, the oxide film becomes thinner with increasing Al content. Nevertheless, Mg and Al oxide growing with the cycling film will block the electron transfer on the electrode surface so that the discharge capacity decreases strongly even after the second cycle.

However, all surface coatings on the amorphous alloy with those three elements may not endure longer charge–discharge cycling in strong alkaline solution. Therefore, it is said that the coating method can be used only in limited extent due to the gradually disappearing protection effect.

3.4. Cycle life of quaternary component MgNi-type alloys

Multicomponent alloying is an effective method for improving the cycle life of AB_5 alloys. Accordingly, the general performance of MgNi alloys can be also improved if the surface oxide as the active interface for desirable oxidation–passivation or corrosion properties is created by multialloying. Therefore, the proper balance between corrosion and passivation defines the operating window for the development of a particular alloy [19–21]. Titanium is, to a certain extent, an effective element to improve the cycle life of $Mg_{50}Ni_{50}$ alloys so that Ti partially substitutes Mg. Adjustment of corrosion resistance can be achieved by the addition of elements like Al or Zr, which are more corrosive than Mg. Thereafter, the combined substitution of a small portion of Mg by elements such as Ti, Al and Zr will increase the electrochemical stability of alloys without significantly reducing the hydrogen storage capacity. Based on the above consideration and our experimental results, two alloys, namely $Mg_{42.5}Ti_5Al_{2.5}Ni_{50}$ and $Mg_{42.5}Ti_5Zr_{2.5}Ni_{50}$, were designed. Their cycle lives are plotted together with the cycle life of $Mg_{50}Ni_{50}$ alloy for comparison in Fig. 8. The cycle life of two quaternary amorphous alloys is better than that of $Mg_{50}Ni_{50}$ alloy. For $Mg_{42.5}Ti_5Al_{2.5}Ni_{50}$ alloy, the improvement of cycle life may be attributed to a strong Ti segregation to the surface during cycling. For $Mg_{42.5}Ti_5Zr_{2.5}Ni_{50}$ alloy, the improvement of cycle life is due to Ti segregation on the surface and the following formation of zirconium–titanium mixed oxide layers was penetrated more easily by atomic hydrogen. However, oxides on the alloy surface increase the electrochemical polarization of an electrode and then decrease the discharge capacity. A fundamental study of corrosion-resistant oxides forming on the surface of MgNi-based alloys, based on the knowledge of the microstructure and cycle life, still needs to be performed.

4. Conclusions

The electrochemical properties of amorphous MgNi-based hydrogen storage alloys synthesized by ball milling depend on the milling conditions and alloy composition. In this work, the following experimental results have been obtained.

(1) The initial discharge capacity of $Mg_{50}Ni_{50}$ alloys varies with grinding time in an attrition mill. The maximum discharge capacity of alloys is obtained at an optimum grinding time. However, longer grinding time after formation of the amorphous alloy has only little effect on the cycle life.

(2) The discharge capacity of an amorphous $Mg_{50}Ni_{50}$ alloy electrode increases firstly with increasing discharge rate from 20 to 100 mA/g and then decreases with further increasing discharge rate from 100 to 600 mA/g. This indicates that a maximum capacity exists at a suitable discharge current density. This behavior, which is rarely found in the AB_5 and AB_2-type crystalline electrode alloys, may be explained by a fast degradation during discharge process in strong alkaline solution.

(3) The cycle life of amorphous $Mg_{50}Ni_{50}$ alloys is sensitive to surface properties. For example, Ti coating on the amorphous $Mg_{50}Ni_{50}$ alloy surface prepared by Spex 8000 mill/mixer improves the cycle life at cost of decreasing discharge capacity.

(4) Two quaternary alloys of $Mg_{42.5}Ti_5Al_{2.5}Ni_{50}$ and $Mg_{42.5}Ti_5Zr_{2.5}Ni_{50}$ were designed. Their cycle lives have been improved. The alloying effect can be attributed to an adjustment of the structure of the oxide film on the amorphous alloys.

References

[1] Y.Q. Lei, Y.M. Wu, Q.M. Yang, J. Wu, Q.D. Wang, Z. Phys. Chem., Bd. 183 (1994) 379.
[2] D.L. Sun, Y.Q. Lei, W.H. Liu, J.J. Jiang, Q.D. Wang, J. Wu, J. Alloys Compd. 231 (1995) 621.
[3] T. Kohno, S. Tsuruta, M. Kanda, J. Electrochem. Soc. 143 (1996) L198.
[4] T. Kohno, M. Kanda, J. Electrochem. Soc. 144 (1997) 331.
[5] C. Iwakura, H. Inoue, S.G. Zhang, S. Nohara, J. Alloys Compd. 270 (1998) 142.
[6] S. Nohara, N. Fujita, S.G. Zhang, H. Inoue, C. Iwakura, J. Alloys Compd. 267 (1997) 76.
[7] W.H. Liu, Y.Q. Lei, D.L. Sun, J. Wu, Q.D. Wang, J. Power Sources 58 (1996) 243.
[8] W.H. Liu, Y.Q. Lei, J. Wu, Q.D. Wang, Int. J. Hydrogen Energy 22 (1997) 999.
[9] C. Iwakura, S. Nohara, H. Inoue, Y. Fukumoto, Chem. Commun. (1996) 1831.

[10] D. Sun, M. Latroche, A. Perchern-Guegan, J. Alloys Compd. 257 (1997) 302.
[11] C.S. Wang, Y.Q. Lei, Q.D. Wang, J. Power Sources 70 (1998) 222.
[12] J.H. Nordlien, S. Ono, N. Masuko, J. Electrochem. Soc. 142 (1995) 3320.
[13] Y.Q. Lei, C.S. Wang, X.G. Yang, H.G. Pan, J. Wu, Q.D. Wang, J. Alloys Compd. 231 (1995) 611.
[14] J.-J. Jiang, J. Alloys Compd. (2000) submitted.
[15] L. Zaluski, A. Zaluska, J.O. Strom-Olsen, J. Alloys Compd. 253–254 (1997) 70.
[16] Y. Tsushio, E. Akiba, J. Alloys Compd. 267 (1998) 246.
[17] A. Zuettel, F. Meli, L. Schlapbach, J. Alloys Compd. 231 (1995) 645.
[18] M. Enyo, T. Yanazaki, K. Suzuki, Electrochim. Acta 28 (1983) 89.
[19] J.O. Strom-Oslen, Y. Zhao, D.H. Ryan, J. Less-Common Met. 172–174 (1991) 922.
[20] A. Zuettel, F. Meli, L. Schlapbach, J. Alloys Compd. 231 (1995) 645.
[21] S. Wakao, H. Sawa, H. Nakano, S. Chubachi, M. Abe, J. Less-Common Met. 131 (1987) 311.